DOI 10.1007/s10891-016-1426-4

Journal of Engineering Physics and Thermophysics, Vol. 89, No. 3, May, 2016

EXPERIMENTAL INVESTIGATION OF THE SUPERSONIC FLOW OVER AN AXISYMMETRIC RING CAVITY

S. V. Guvernyuk, A. F. Zubkov, and M. M. Simonenko UDC 533.6.011

This paper presents the results of the experimental investigation of the supersonic flow over a ring cavity of rectangular cross-section on a cylindrical body with a conical tip. The evolution of the flow over a cavity with its continuously changing extent has been investigated. The transition zone boundaries within which both an open and a closed schemes of flow are possible have been determined by the parameter of the relative extent of the cavity. It has been shown that the flow conditions in the transition zone depend on the prehistory of the flow. The main stages of cavity flow restricuting at the transition zone boundaries have been described.

Keywords: *ring cavity, supersonic flow, flow separation, hysteresis.*

Introduction. The supersonic flow over rectangular cavities was investigated experimentally and numerically in [1–12]. Depending on the ratio of the length of the cavity L to its depth h, two different flow schemes are possible [1, 2]. If $\lambda = L/h$ is small ($\lambda < \lambda_O$), an open cavity is formed. In this case, throughout the region of the cavity a subsonic circulatory flow 1 separated from the external supersonic flow by a mixing layer 2 is initiated (Fig. 1a). If λ exceeds some critical value ($\lambda > \lambda_C$), then a closed cavity is realized (Fig. 1b). In this case, in the cavity two isolated separation regions are formed, one of which (region 3) is formed behind the front step and the other (region 4) is formed behind the rear step. In the external supersonic flow field, shock waves arise thereby: a compensation shock 5 ahead of the front separation region and a shock 6 ahead of the rear separation region. The range $\lambda_O < \lambda < \lambda_C$ corresponds to the so-called transition region for which there is an additional classification of flow schemes [1–4].

The character of the supersonic cavity flow depends also on the state of the boundary layer at the cavity inlet and the Mach M and Reynolds Re numbers. For plane cavities of rectangular cross-section in supersonic turbulent flow in the range of moderate Mach numbers M = 2–4, there are empirical estimates of the boundaries of regions in which a particular flow scheme is realized: $\lambda_O = 10$, $\lambda_C = 13$. The results of experimental and numerical studies of the supersonic flow over axisymmetric cavities of rectangular cross-section on cylindrical bodies [5–11] are in good agreement with the data for plane cavities. Similarity of results connected with the collapse of plane, axisymmetric, and even free cavities is observed [13].

Assuming that with decreasing λ the closed cavity opens when the separation regions localized behind the front step and ahead of the rear step come in contact with each other, the cavity collapse criterion was formulated; according to this criterion, the critical length of the cavity is equal to the total length of the above separation regions [1]. However, this criterion gives underestimated values [3], and therefore it was suggested [4] to take into account the correction for the total length of compression regions near the front and rear separation regions in the cavity. The presence of a hysteresis expressed as the dependence of the critical length on whether the change of one flow regime to another took place with decreasing or increasing λ was noted [3].

In experimental investigations of the supersonic flow over ring cavities in the transition region [8], it was established that the open scheme of flow is more stable to external disturbances, whereas the closed scheme can easily change to the open scheme under insignificant short-time actions. In particular, in the transition region small changes in the angle of incidence led to an irreversible change of the initially closed scheme of flow to an open one, after which the open scheme recovered upon any finite changes in the angle of incidence and subsequent return of the model to the initial state. The length of the hysteresis region depends on the angle of incidence and the Mach number of the incident flow, as well as on the flow forming conditions upstream of the inlet to the cavity determined by the geometry of the front tip [9].

Research Institute of Mechanics, M. V. Lomonosov Moscow State University, 1 Michurinskii Ave., Moscow, 119192, Russia; email: sim1950@mail. ru. Translated from Inzhenerno-Fizicheskii Zhurnal, Vol. 89, No. 3, pp. 670–679, May–June, 2016. Original article submitted April 30, 2015.

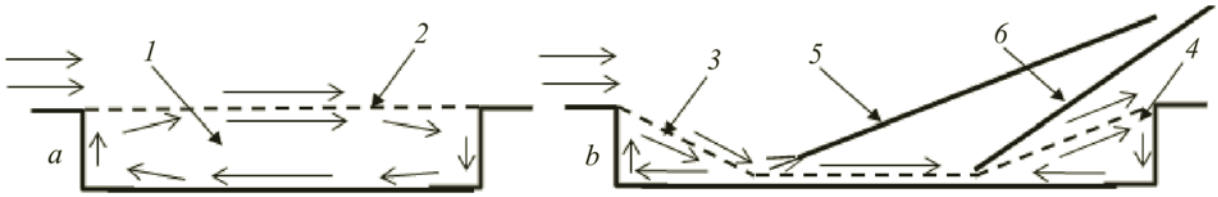

Fig. 1. Open (a) and closed (b) schemes of flow over the cavity.

Various active and passive methods of controlling the flow in cavities were investigated [14–19]. The main aim was to decrease loads on the structure by forced holding of the open scheme of flow, as well as to lower the noise level generated by the cavity. Consideration was given to the question of the simultaneous supersonic flow over cavities in tandem [20–22], the possibilities of using cavities for fuel and oxidizer mixing in supersonic flow were explored [23, 24], and the features of the supersonic flow over cavities were investigated [25]. Placing forward and backward protruding coaxial disks on cylindrical bodies [26] also leads to the formation of original ring cavities, the flow over which can be open or closed.

In spite of the large number of experimental and numerical works devoted to the investigation of the supersonic flow over cavities, the physics of the flow even in the simplest rectangular cavity is still not clearly understood. In particular, the question which flow scheme, open or closed, will be realized in the transition region (hysteresis region) under the same initial conditions is still open. The processes of change of the regimes of flow over the cavity are still not clearly understood. These questions are of not only fundamental, but also of practical importance in both choosing optimal schemes of flow over bodies with cavities and in developing new methods for controlling the flow in the cavity.

This paper presents the results of experimental investigations of the supersonic axisymmetric flow over a transverse ring cavity of rectangular cross-section on a cylindrical body with a conical tip under continuous variation of the cavity length in the flow. The aim of the paper was to investigate the features of the supersonic flow over a cavity of varying length under different conditions of flow formation ahead of the cavity determined by the geometry of the front tip with account for the nonstationary processes at the stage of change of flow regimes due to the change of schemes of flow over a ring cavity.

Experimental Model and Testing Conditions. The experimental model is schematically represented in Fig. 2. The model included a cylindrical case 1 of diameter $D = 45$ mm. On the case 1, a cylindrical rod 2 of diameter $d = 29$ mm was mounted coaxially with it. The rod 2 can reciprocate relative to the case 1 along the symmetry axis. At the free end of the rod 2 a separable conical tip 3 with a half-opening β was set. The gap between the case 1 and the tip 3 represents a ring cavity with equal heights $h = 8$ mm of the front and the rear steps. The length L of the cavity can be both decreased and increased at the expense of longitudinal displacements of the rod 2 relative to the case 1.

Experiments were carried out in the A-7 wind tunnel of the Research Institute of Mechanics of the Moscow State University. This wind tunnel has a closed working section of square cross-section of size 0.6×0.6 m^2 and length 1.5 m. Blocking of the working section with the model did not exceed 5%. The working medium was air with a stagnation temperature of 270–275 K. The total pressure of the flow and the Mach number in the working section of the wind tunnel were, respectively, $P_0 = 4.3 \cdot 10^5$ Pa and M = 3.0. The unit Reynolds number calculated by the flow parameters in the working section of the wind tunnel $\mathrm{Re}_1 = 3.7 \cdot 10^{-7}$ m^{-1}.

The experimental model was set on the bottom sting at a zero angle of incidence. Video recording of schlieren images of flow patterns in digital format was carried out. To visualize the flow structure, an IAB-451 standard shadow device was used. The pressure in the working section of the wind tunnel and on the rear step of the cavity at a distance of ~h/2 from the cavity bottom was registered, and the pressure transducers were located outside the working section of the wind tunnel and connected to the pressure heads by flexible pipes of length up to 3 mm. MP3H6115A-type piezoelectric sensors with a measurement range of 15–115 kPa were used. The pressure measurement error did not exceed ±1.5%. Because of the large lenght of the air path, the high-frequency pressure fluctuations were smoothed, and actually the time-averaged static pressure ahead of the rear step was registered. To measure the total pressure in the settling chamber of the wind tunnel, MPX5500-type pressure transducers were used.

The minimum initial settling length of the cavity was $L = L_{\min} = 53$ mm ($\lambda_{\min} = 6.625$). Upon each start after the steady-state flow regime in the working section of the wind tunnel was reached, the cavity length was varied continuously first in the direction of increasing values up to $L_{\max} = 117$ mm ($\lambda_{\max} = 14.6$) and then in the direction of decreasing values

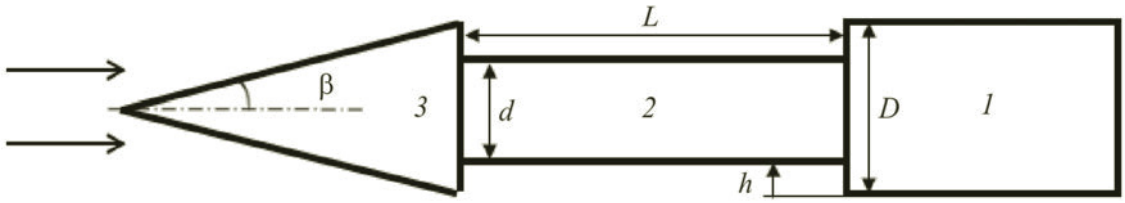

Fig. 2. Scheme of the experimental model: 1) cylindrical case; 2) rod; 3) conical tip.

TABLE 1. Flow Parameters on the Surface of the Front Tip and at the Cavity Inlet

Model	β,°	S_c, m	$Re_{S1}\cdot10^{-7}$, м$^{-1}$	$Re_S\cdot10^{-6}$	$Re\cdot10^{-6}$	M_e	s_t	δ_c, mm
1	10	0.1296	4.3	5.6	4.8	2.7	0.5–0.8	1.5
2	20	0.0658	4.9	3.2	2.4	2.3	0.8–1.3	1.4
3	30	0.0450	4.9	2.2	1.7	1.8	1.2–1.9	1.4

down to the initial state. The rate of change in the cavity length reached 2 mm/s. The instantaneous length of the cavity was determined by the video recording data of schlieren images.

We investigated three models differing in the form of the front tip (β = 10, 20, and 30°). Table 1 presents for each model the unit Reynolds numbers Re_{S1} calculated by the flow parameters on the cone of the front tip, as well as the corresponding current Reynolds numbers Re_S and Re of the flow at the inlet to the cavity and the Mach numbers M_e of the nonviscous flow on the cone surface. For wind tunnels, there are empirical estimates of Reynolds numbers corresponding to the beginning of turbulent transition on the surface of a sharp cone depending on M_e [27], Re_S [28], and Re [29]. On the basis of the data for our experimental conditions, we made a corresponding estimate of the beginning of the region of turbulent transition on the used cones. Table 1 gives for each model the range of values of the quantities $s_t = S_t/S_c$, where S_t is the distance to the transition region counted off from the vertex of the cone, $S_c = 0.5D/\sin\beta$. As $s_t < 1$ (model 1), a turbulent transition should ensue on the surface of the cone of the front tip, and the flow at the cavity inlet is expected to be turbulent. As $s_t > 1$ (model 3) the flow at the cavity inlet is expected to be laminar. In the case of model 2, the calculated distance to the turbulent transition region is comparable to the length of the formed cone, a turbulent transition can ensue on the surface of the cone of the front tip, just ahead of the cavity inlet, or the flow at the cavity inlet will be laminar. Assuming that there is no turbulization of the flow on the cone, we estimated the thickness of the laminar boundary layer at the inlet to the cavity δ_c, the obtained data are given in Table 1.

Test Data and Analysis. *Flow structure in the cavity*. At the minimum setting length of the cavity $\lambda = \lambda_{min}$ after the wind tunnel begins to operate, the open flow scheme was always realized. After the flow over the model reached the steady state, the cavity length was continuously increased to $\lambda = \lambda_{max}$, and for a certain value of $\lambda = \lambda_C$ in the range of $\lambda_{min} < \lambda < \lambda_{max}$ the flow regime always switched to the closed scheme. When $\lambda = \lambda_{max}$ was reached, the cavity length was continuously decreased to the initial value, and always at some $\lambda = \lambda_O$ the flow regime switched back to the previous one. In the range of $\lambda_O < \lambda < \lambda_C$ at the same values of λ both the open and the closed schemes of flow were realized.

The shadow photographs in Fig. 3 illustrate the open (a, b) and the closed (c, d) schemes of flow over the cavity at the minimum (a, b) and maximum (c, d) values of the relative length of the cavity λ admitting the existence of both flow schemes. The photographs in Fig. 3a and b were taken with continuously increasing length of the open cavity, and those shown in Fig. 3c, d were taken with continuously decreasing length of the closed scheme. We can clearly see the attached bow shock 1 arising ahead of the conical tip (β = 20°) and the leading front 2 of the rarefaction wave set up due to the expansion of the flow behind the front edge of the cavity.

In the regimes with the open scheme of flow (Fig. 3a, b), the trailing front 3 of the rarefaction wave and the mixing layer 4 extending from the front step down the stream are observed. The mixing layer separates the subsonic detached circulatory flow in the cavity from the external supersonic flow. The flow in the open cavity and in its adjoining supersonic region depends on λ, since disturbances from the rear step are transferred forward, as λ changes, along the full length of the separation region. The angle (with the cavity bottom) of the observed trailing front 3 of the rarefaction wave decreases with

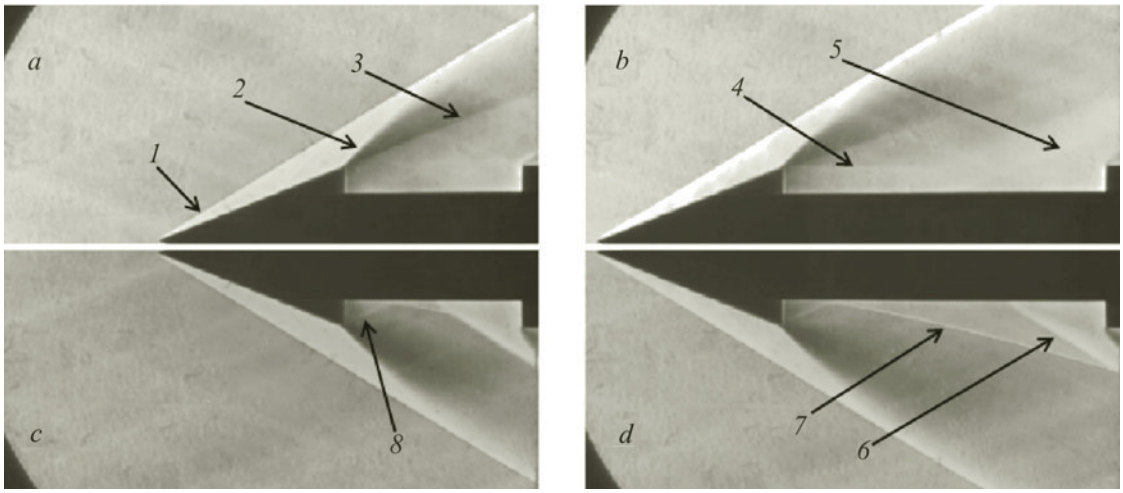

Fig. 3. Visualization of the structure of the flow over the cavity for the open (a, b) and the closed (c, d) flow schemes at $\beta = 20^o$; $\lambda = 7.0$ (a, c) and $\lambda = 13.2$ (b, d), the supersonic flow is directed from left to right.

increasing λ, which means a larger expansion of the flow in the rarefaction wave on the front step and, accordingly, a decrease in the pressure in the separation region. At the same time, with increasing λ, the appearance of compression waves 5 in the supersonic region of the flow ahead of the rear step is observed, which should lead to an increase in the local pressure in the separation region.

In the case of the closed cavity (Fig. 3c, d), two shock waves 6 and 7, as well as the boundary 8 of the separation region behind the front step, are observed. The shock 6 is located immediately ahead of the separation region near the rear step of the cavity (the photographs do not show the boundary of the separation region ahead of the rear step), on which stagnation of the supersonic flow propagating along the cavity bottom occurs. The compensation shock 7 is initiated in the vicinity of the juncture of the supersonic flow and the cavity bottom and extends downstream in the region of expansion of the supersonic flow. On this shock, the expanded supersonic flow stagnates and makes a turn along the cavity bottom. In the closed cavity, the front and rear separation regions are separated by the supersonic flow and do not interact. The flow behind the front step down the stream up to the shock 6 does not depend on λ and is determined exclusively by the flow parameters at the cavity inlet. At the same time the flow parameters ahead of the rear step of the cavity vary with λ. At large λ the shock 6 intersects with the shock 7 outside the region of the cavity and just below its rear step. With decreasing λ the intersection point of the shocks 6 and 7 moves along the shock 7 up the stream and approaches the bottom of the cavity.

Hysteresis due to the change in the cavity length. When the cavity length is increased continuously from the initial value of $\lambda = \lambda_{min}$ to $\lambda = 13.2$, the initially open scheme does not change (Fig. 3a, b). When $\lambda = \lambda_C = 13.2$ is reached, a sudden change in the flow structure in the cavity takes place and a closed scheme of flow is formed (Fig. 3d). As λ is further increased to the limiting value in the experiment $\lambda_{max} = 14.2$, the closed scheme of flow remains unchanged. As λ is then decreased continuously, the closed scheme of flow over the cavity remains unchanged up to $\lambda = 7.0$ (Fig. 3c), and at $\lambda = \lambda_O = 7.0$ it changes as suddenly to the open scheme (Fig. 3a). The length of the transition region, in which both the open and the closed schemes of flow are observed, in the considered example ($\beta = 20^o$) was $\Delta\lambda = \lambda_C - \lambda_O = 6.2$, or 50.4 mm in absolute units.

Comparison of the results of visualization of the flow structure and the measurement data of the cavity pressure confirms that the region of $\lambda_O < \lambda < \lambda_C$ is a typical region of hysteresis along the cavity length. All other things being equal, the observed flow structure in this region depends on what flow structure preceded the change in λ. Figure 4 shows the characteristic hysteresis curves for the cavity pressure. They reflect the change in the relative pressure *P* ahead of the rear step of the cavity with continuously increasing or decreasing λ for various angles β of the conical tip. The lower branches of the curves in Fig. 4 show the increase in λ, and the upper branches show the decrease in λ. The pressure *P* is the mean value of pressures at the measurement points on the rear step and is referred to the static pressure in the flow.

With increasing λ of the initially open cavity, the pressure *P* on the rear step increases monotonically, which agrees with the results of visualization pointing to the appearance of a system of compression waves in the supersonic flow in the region ahead of the rear step of the cavity. As it turned out, the value, as well as the character of the pressure change

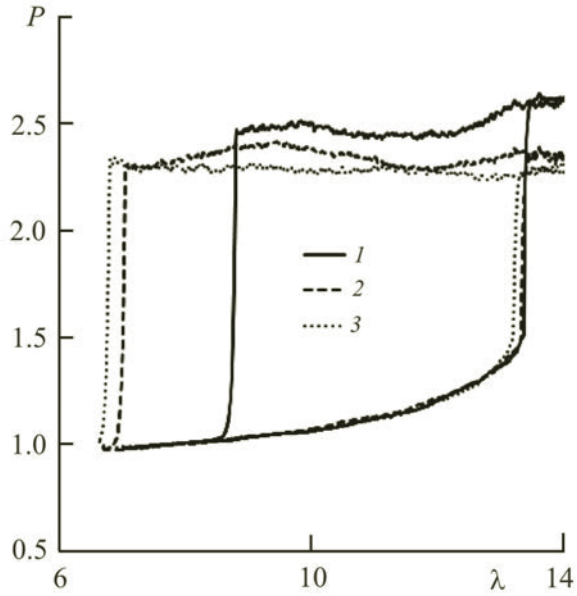

Fig. 4. Dependence of the relative pressure P on the rear step of the cavity on the cavity length λ at various half-openings of the tip of the models: 1) $\beta = 10^{o}$; 2) 20; 3) 30.

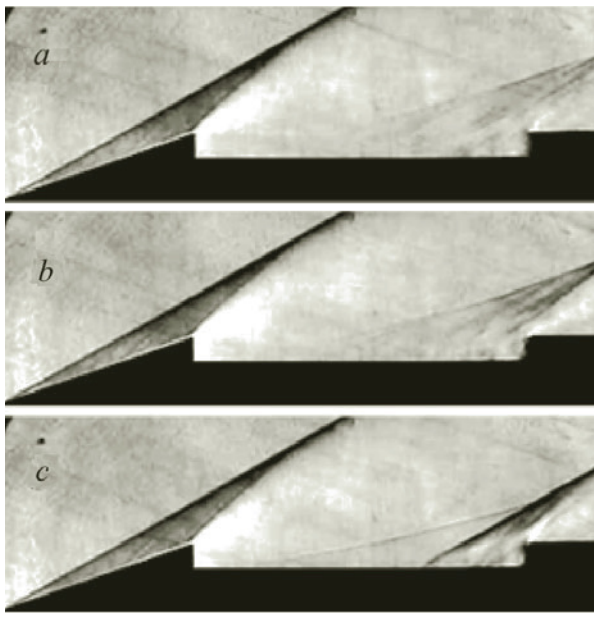

Fig. 5. Closing kinematics of the open cavity in the vicinity of λ = 13.2, the interval between shots is $\Delta t = 6 \cdot 10^{-4}$ s.

on the rear step of the open cavity are practically independent of the angle β. For all models, to the short cavity there corresponds $P < 1$, at $\lambda = 8$ $P = 1$ is attained, and the maximum value of $P = 1.5$ corresponds to the maximum length $\lambda = \lambda_C$ of the open cavity. When $\lambda = \lambda_C$ is attained (slightly differing for various angles β) the cavity collapses with a stepwise increase in P. After the cavity collapses at $\lambda > \lambda_C$, the pressure ahead of the rear step is different for different conical tips. With increasing β, the pressure P decreases, which can be explained by the increase in the loss of the total pressure of the flow on the shock waves. As λ is further increased upon restructuring, the high pressure ahead of the rear step of the closed cavity remains unchanged.

With decreasing λ of the closed cavity the pressure on the rear step varies nonmonotonically, remaining high up to some value of $\lambda = \lambda_O$ depending on β. The relative deviation of the pressure value ahead of the rear step of the closed

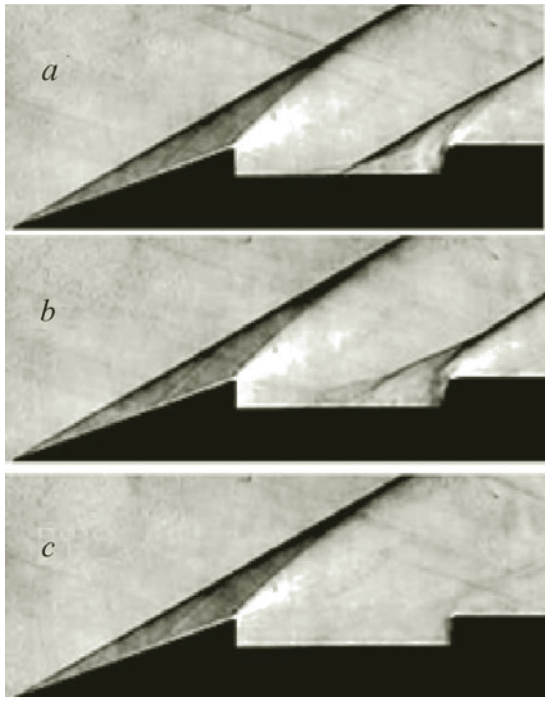

Fig. 6. Opening kinematics of the closed cavity in the vicinity of $\lambda = 7.0$, the interval between shots is $\Delta t = 6 \cdot 10^{-4}$ s.

cavity from the mean value throughout the range $\lambda_O < \lambda < \lambda_C$ did not exceed 3, 2, and 1.5% for angles $\beta = 10$, 20, and 30°, respectively. When $\lambda = \lambda_O$ is reached, the cavity opens, and the pressure ahead of its rear step sharply decreases and reaches the value (at the same λ) corresponding to the pressure on the lower branch of the hysteresis curve (Fig. 4). The subsequent change in P with decreasing λ takes place along the lower branches of the above curves. The quantitative values of the quantities λ_O and λ_C for various β are given below.

Restructuring of flows in the cavity. The collapse process of the open cavity at $\lambda = \lambda_C$ is illustrated by the shadow photographs of the flow fields shown in Fig. 5. As mentioned above, the high pressure ahead of the rear step of the open cavity leads to the formation of a system of compression waves in the external supersonic flow (Fig. 5a). With increasing λ the pressure ahead of the rear step increases, the pressure disturbances are transferred upstream in the subsonic saturation region, the intensity of compression waves in the external supersonic flow field increases, and the mixing layer is forced against the cavity bottom (Fig. 5b). At $\lambda = \lambda_C$ the system of compression waves ahead of the rear step transforms into two shock waves (Fig. 5c), and the single circulation region breaks down into two regions, one of which is formed behind the front step, and the other ahead of the rear step of the cavity. The collapse process of the cavity is completed with a sharp increase in the pressure ahead of the rear step at $\lambda = \lambda_C$ (Fig. 4).

In the closed cavity, as the λ decreases, the separation regions localized near the front and the rear step approach each other. At $\lambda > \lambda_O$ the flow parameters and structure behind the front step remain unchanged, and the conditions of flow around the rear step change because of the transverse and longitudinal inhomogeneities of the incident flow caused by the presence of a compensation shock wave in the flow field (Fig. 5c and Fig. 6a). When a certain value of $\lambda = \lambda_O$ is reached, the front and the rear separation regions in the closed cavity begin to interact (Fig. 6b), which leads to pressure equalizing in these regions and the formation of a single mixing layer between the steps of the open cavity. This process is accompanied by the disappearance of shock waves from the external flow field (Fig. 6c) and a sharp decrease in the pressure ahead of the rear step of the cavity to the value corresponding to the pressure in the open cavity.

The described restructuring of the flow in the cavity occurs in a short time (less than 10^{-3} s). At the same time the process of open cavity collapse is preceded by a longer process of the formation of a system of compression waves in the supersonic flow ahead of the rear step. The collapse length of the cavity λ_C changed slightly from experiment to experiment, the deviation from the mean value did not exceed 2%, and the deviation of λ_O reached 6%. A possible reason for the more substantial spread of the λ_O values is the increase in the intensity of three-dimensional pulsations in the flow ahead of the

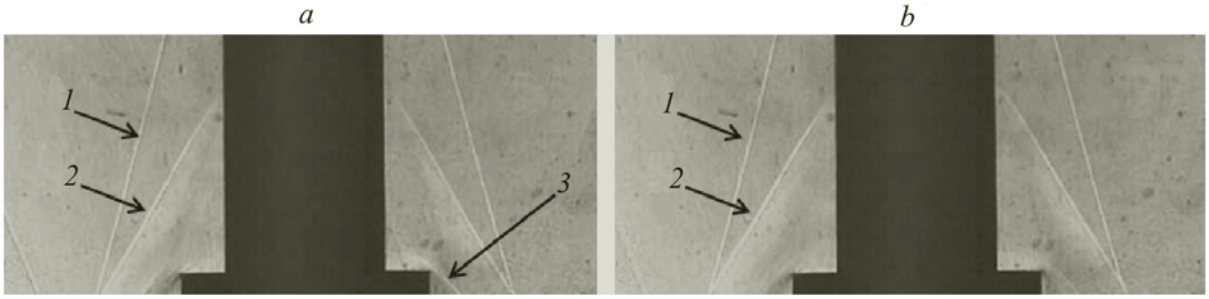

Fig. 7. Visualization of the structure of the flow over the rear step of the closed cavity at $\beta = 30^{o}$; $\lambda = 13.2$ at various instants of time (the interval between shots is $2 \cdot 10^{-4}$ s).

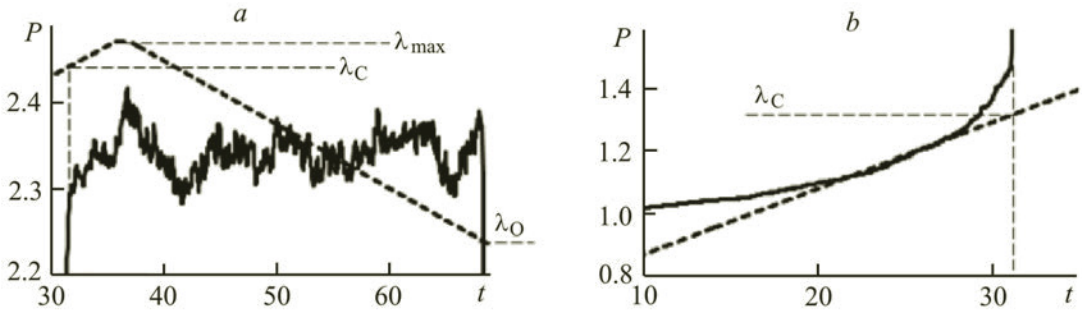

Fig. 8. Change with time in the pressure ahead of the rear step of the closed (a) and the open (b) cavities at $\beta = 30^{o}$.

rear step of the closed cavity, which leads to some uncertainty of the onset of interaction of the separation regions and, accordingly, of the moment of opening of the closed cavity with its continuously varying length.

Flow pulsations in the closed cavity. Pressure fluctuations ahead of the rear step of the closed cavity are due to the nonstationary character of the flow near the rear step. Figure 7 shows the shadow photographs of the flow field near the rear step of the closed cavity obtained at 0.0002 s intervals. Figure 7a clearly shows the compensation shock 1, the shock 2 ahead of the separation region, as well as the shock 3 immediately ahead of the rear edge of the cavity. In the following photograph (Fig. 7b) the shock 3 is no longer observed. This points to the presence of transverse pulsations of the flow in the separation region accompanied by the appearance of nonstationary local supersonic zones ahead of the rear step. Along with this, the vertex of the shock 2 oscillates about some mean position. One possible reason for the above pulsations is the instability of the mixing layer separating the separation region localized near the rear step of the cavity from the external flow. The joining of the mixing layers with the rear step of the cavity should be accompanied by a local increase in the pressure, which is turn promotes the inverse process of detachment of this layer and a decrease in the pressure. This oscillation process is complicated by the nonstationary character of the interaction of the shock 2 with the boundary layer propagating along the bottom of the cavity, as well as by the spatial character of the flow as a consequence of the transfer of disturbances throughout the subsonic ring separation region.

Pulsations of the flow structure near the rear step of the closed cavity affect the character of the pressure change. While a change in λ leads to a smooth variation of the pressure along the lower branches of the curves (open cavity), on the upper branches of the curves (closed cavity) marked pressure oscillations are observed (Fig. 4). Figure 8 scales up the graphs of the variation in time of the pressure at one of the measurement points on the rear step in the cases of the closed (a) and open (b) cavities. The continuous variation in time of the cavity length λ taking place thereby is shown by a dashed curve on which the values corresponding to the attainment of λ_{max}, λ_C, and λ_O are marked. The pressure pulsation frequency ahead of the rear step of the closed cavity reached 10 Hz. It should be noted that higher-frequency pulsations of the flow are smoothed by the air path of the pressure measuring system.

Influence of the opening of the conical tip. In all experiments with different models, the hysteresis region was localized in the range of $\lambda_{min} < \lambda < \lambda_{max}$. Table 2 gives the values of λ_C, λ_O, and $\Delta\lambda$ defining the boundaries and length of the

TABLE 2. Characteristic Length of the Separation Regions in the Closed Cavity

Model	β,°	λ_C	λ_O	$\Delta\lambda$	λ_{Fmin}	λ_{Fmax}	λ_D	$\lambda_{Fmin} + \lambda_D$	$\lambda_{Fmax} + \lambda_D$	$\Delta\lambda_1$	$\Delta\lambda_2$
1	10	13.4	8.8	4.6	3.9	4.0	1.8	5.7	5.8	3.1	7.6
2	20	13.3	7.0	6.3	3.4	4.0	2.0	5.4	6.0	1.6	7.3
3	30	13.2	6.9	6.3	3.3	4.0	2.0	5.3	6.0	1.6	7.3

hysteresis region for various values of β averaged over a series of experiments. While the upper boundary λ_C weakly depends on β, the lower boundary λ_O and, accordingly, the length of the transition region differ markedly for the considered values of β. The upper boundary of the transition region is thereby in good agreement with the known data [1–12], and the lower boundary turned out to be much lower than the value of $\lambda_O = 10$ predicted in the literature.

The lower value of the quantity λ_O in the present experiments is explained by the smaller extent of the separation region behind the inverse step on the conical wall compared to such a step on a cylindrical or a flat wall. In the latter case, the extent of the turbulent plane or axisymmetric near wake behind the step is 4–5 units of its height [12], and in our case of the inverse step on the cone, these values are 1.8, 2.0, and 2.0 at $\beta = 10$, 20, and 30^o, respectively. Thus, the extent λD of the separation region behind the inverse step on the conical surface turned out to be almost twice smaller than the extent of such a region behind the step on a cylindrical or a flat wall.

It should be noted that the length of the front separation region was estimated by the visible boundary of the mixing layer and this quantity was practically independent of λ. The length of the rear separation region was estimated visually by the distance of withdrawal of the shock wave ahead of the rear step, and this quantity varies with λ. The maximum value of $\lambda_{Fmax} = 4$ is attained near the upper boundary of the transition region at $\lambda = \lambda_C$. As λ decreases, the length of the rear separation region decreases and at $\lambda = \lambda_O$ it is equal to $\lambda_{Fmin} = 3.9$, 3.4, and 3.3 for $\beta = 10$, 20, and 30^o, respectively.

The observed increase in λ_O at $\beta = 10$ is due to the thicker boundary layer at the inlet to the cavity, which is due to the turbulent transition in the boundary layer on the surface of the conical tip. The thicker boundary layer ahead of the cavity inlet leads to a thickening of the mixing layer and, accordingly, to a thickening of the boundary layer behind the front separation region of the closed cavity. As a consequence, the region of influence behind this separation increases. The data presented in Table 2 characterize the main geometric parameters of the separation regions for all tested models. The length of the influence region behind the front separation was determined to be the minimum possible distance between the front and the rear separation regions in the closed cavity $\Delta\lambda_1 = \lambda_O - (\lambda_{Fmin} + \lambda_D)$ at $\lambda = \lambda_O$. The maximum distance between the front and the rear separation regions $\Delta\lambda_2 = \lambda_C - (\lambda_{Fmax} + \lambda_D)$ is attained for the hysteresis range at $\lambda = \lambda_C$.

The foregoing permits concluding that the critical length of the closed cavity λ_O corresponding to the lower boundary of the hysteresis region is equal to the sum of the lengths of the front and the rear separation regions in the closed cavity with account for the correction for the length of the influence region behind the front separation region. The value of this correction depends on the state of the boundary layer at the inlet to the cavity. The collapse length λ_C of the open cavity corresponding to the upper boundary of the hysteresis region is thereby practically independent of the conditions of flow formation at the cavity inlet. This agrees with the known data obtained in a wide range of Mach and Reynolds numbers.

Conclusions. We have simulated experimentally the phenomenon of aerodynamic hysteresis in axisymmetric supersonic flow over a conical-cylindrical body with a transverse ring cavity adjoining the kink of the generating line of the body. By means of the technology of continuously increasing or decreasing the relative length of the cavity in the flow, the ranges of parameters, in which both the open and the closed schemes of flow over the cavity are observed have been determined. It has been shown that a concrete type of the realized flow regime in the transition region depends on the flow prehistory. A classification of the main stages of restructuring of flows over the cavity at the hysteresis boundaries along the cavity length is given. The lower boundary strongly depends on the state of the boundary layer ahead of the cavity inlet determined under the given conditions by the half-opening of the front conical tip. In contrast, the upper boundary of the hysteresis region is practically insensitive to a change in the conditions at the inlet to the cavity. The minimum value of the relative length of the closed cavity preceding its opening has been determined as the sum of the lengths of the front and the rear separation regions with allowance made for the correction for the length of the influence region behind the front separation.

This work was supported by the Russian Foundation for Basic Research (grant No. 15-01-99623).

NOTATION

D, external diameter of the ring cavity, m; *d*, internal diameter of the ring cavity, m; *h*, height of the cavity, m; *L*, length of the cavity, m; M, M_e, Mach numbers; *P*, relative pressure; Re, Re_S, Reynolds numbers; Re_1, Re_{S1}, unit Reynolds numbers, m^{-1}; *S*, distance along the generating line counted off from the cone vertex, m; S_c, length of the generating line of the tip, m; S_t, distance to the turbulent transition region, m; *s*, relative length; β, half-opening of the conical tip, m; δ, boundary layer thickness, m; λ, relative length of the cavity ($\lambda = L/h$); λ_C, upper boundary of the transition region; λ_D, length of the front separation region; λ_F, length of the rear separation region; λ_O, lower boundary of the transition region. Subscripts: max, min, maximum and minimum values; 0, stagnation parameters.

REFERENCES

1. A. F. Charwat, J. N. Roos, F. C. Dewey, and J. A. Hitz, An investigation of separated flows. Part I: The pressure field, *J. Aerosp. Sci.*, **28**, No. 6, 457–470 (1961).
2. A. F. Charwat, C. F. Dewey, J. N. Roos, and J. A. Hitz, An investigation of separated flows. Part II: Flow in the cavity and heat transfer, *J. Aerosp. Sci*., **28**, No. 7, 513–527 (1961).
3. R. L. Stalling and F. J. Wilcox, *Experimental Cavity Pressure Distribution at Supersonic Speeds*, NASA TP 2683 (1987).
4. J. Zhang, E. Morishita, T. Okunuki, and H. Itoh, Experimental investigation on the mechanism of flow-type changes in supersonic cavity flows, *Trans. Jpn. Soc. Aeronaut. Space Sci.*, **45**, No. 149, 170–179 (2002).
5. M. G. Morozov, Similarity of supersonic separation zones, *Izv. Akad. Nauk SSSR*, *Mekh. Zhidk. Gaza*, No. 6, 115–118 (1970).
6. V. I. Penzin, Separation flow in a ring groove, *Uch. Zap. TsAGI*, **VII**, No. 6, 124–130 (1976).
7. A. I. Shvets, Investigation of the flow in a cylindrical recess on an axisymmetric body in supersonic flow, *Izv. Ross. Akad. Nauk*, *Mekh. Zhidk. Gaza*, No. 1, 123–131 (2002).
8. S. V. Guvernyuk, A. F. Zubkov, M. M. Simonenko, and A. I. Shvets, Experimental investigation of the three-dimensional supersonic flow over an axisymmetric body with a ring cavity, *Izv. Ross. Akad. Nauk*, *Mekh. Zhidk. Gaza*, No. 4, 136–142 (2014).
9. S. V. Guvernyuk, A. F. Zubkov, and M. M. Simonenko, On the observation of the aerodynamic hysteresis in supersonic flow over a ring cavity on an axisymmetric body, in: *Advances in the Mechanics of Continuous Media*, Collected papers at the Int. Conf. timed to the 75th birthday of Academician V. A. Levin, OOO "Megaprint," Irkutsk (2014), pp. 163–168.
10. K. Mohri and R. Hillier, Computational and experimental study of supersonic flow over axisymmetric cavities, *Shock Waves*, **21**, No. 3, 175–191 (2011).
11. A. D. Savel′ev, Numerical simulation of the supersonic flow over extended grooves, *Uch. Zap. TsAGI*, **XLII**, No. 3, 60–72 (2011).
12. S. J. Lawson and G. N. Barakos, Review of numerical simulations for high-speed, turbulent cavity flows, *Prog. Aerosp. Sci.*, **47**, No. 3, 186–216 (2011).
13. P. K. Chang, *Separation of Flow*, Pergamon Press, Oxford (1970).
14. F. Wilcox Jr., Tangential, semisubmerged, and internal store carriage and separation at supersonic speeds, *AIAA Paper*, 91-0198 (1991).
15. L. N. Cattafesta, D. R. Williams, C. W. Rowley, and F. S. Alvi, Review of active control of flow-induced cavity resonance, *AIAA Paper*, 2003-3567 (2003).
16. L. N. Cattafesta, Q. Song, D. R. Williams, C. W. Rowley, and F. S. Alvi, Active control of flow-induced cavity oscillations, *Prog. Aerosp. Sci*., **44**, No. 7, 479–502 (2008).
17. N. Zhuang, F. S. Alvi, M. B. Alkislar, and C. Shih, Supersonic cavity flows and their control, *AIAA J*., **44**, No. 9, 2118–2128 (2006).
18. J. Zhang, E. Morishita, T. Okunuki, and H. Itoh, Control of closed-type supersonic cavity flows, *ICAS2002 CONGRESS*, 393.1–393.8 (2002).
19. N. S. Vikramaditya and J. Kurian, Experimental study of influence of trailing wall geometry on cavity oscillations in supersonic flow, *Exp. Therm. Fluid Sci*., **54**, 102–109 (2014).
20. X. Zhang and J. A. Edwardst, Experimental investigation of supersonic flow over two cavities in tandem, *AIAA J*., **30**, No. 5, 1182–1190 (1992).

21. N. Taborda, D. Bray, and K. Knowle, Experimental investigation into transonic flows over tandem cavities, *Aeronaut. J.*, **105**, No. 1045, 119–124 (2001).
22. V. N. Zaikovskii, Ya. I. Smul′skii, and V. M. Trofimov, Influence of tandem cavities on the heat transfer in a supersonic flow, *Teplofiz. Aéromekh*., No. 3, 423–430 (2002).
23. T. Mathur, M. Gruber, K. Jackson, J. Donbar, W. Donaldson, T. Jackson, and F. Billig, Supersonic combustion experiments with a cavity-based fuel injector, *J. Propuls. Power*, **17**, No. 6, 1305–1312 (2001).
24. T. Ukai, H. Zare-Behtash, E. Erdem, K. H. Lo, K. Kontis, and S. Obayashi, Effectiveness of jet location on mixing characteristics inside a cavity in supersonic flow, *Exp. Therm. Fluid Sci*., **52**, 59–67 (2014).
25. R. C. Palharini and T. J. Scanlon, Aerothermodynamic comparison of two- and three-dimensional rarefied hypersonic cavity flows, *J. Spacecraft Rockets*, **51**, No. 5, 1619–1630 (2014).
26. S. A. Isaev, Yu. M. Lipnitskii, A. N. Mikhalev, A. V. Panasenko, and A. E. Usachov, Simulation of the supersonic turbulent flow over a cylinder with coaxial disks, *J. Eng. Phys. Thermophys*., **84**, Issue 4, 827–839 (2011).
27. M. R. Malik, Prediction and control of transition in supersonic and hypersonic boundary layers, *AIAA J.*, **27**, No. 11, 1487–1493 (1989).
28. V. Ya. Borovoi, Yu. Yu. Kolochinskii, and L. V. Yakovleva, Investigation of the influence of the unit Reynolds number on the boundary layer transition on a sharp cone, *Izv. Akad. Nauk SSSR*, *Mekh. Zhidk. Gaza*, No. 4, 32–38 (1982).
29. A. A. Maslov and S. G. Shevel′kov, Features of the laminar boundary layer transition on a cone, *Izv. Akad. Nauk SSSR*, *Mekh. Zhidk. Gaza*, No. 6, 23–27 (1985).